ADVANCED OPTICAL MATERIALS
www.advopticalmat.de

Size- and Shape-Dependent Fluorescence Quenching of Gold Nanoparticles on Perylene Dye

*Chenming Xue, Yuhua Xue, Liming Dai, Augustine Urbas, and Quan Li**

Organo-soluble decane thiol monolayer-protected gold nanoparticles of different shapes and sizes are homogenously mixed with strong fluorescent perylene diimide (PDI) dye molecules in both solution and solid states. The effect of the doped gold nanoparticles on PDI is investigated by UV–vis, fluorescence, transmission electron microscopy, scanning electron microscopy, and Raman experiments. The gold nanoparticles are found to modify the strong fluorescence properties of PDI depending on particle size and shape. The smallest spherical gold nanoparticles (2.6 nm) exhibit the strongest quenching effect. When the smallest spherical gold nanoparticles are cast on the PDI soaked paper followed by drying and/or sealing in a polydimethylsiloxane film, the area with gold nanoparticles shows significant quenching effects under a UV light but appears visually identical to the surrounding area under daylight. This demonstrates the potential to introduce gold nanoparticles into practical applications such as antifraud technologies.

1. Introduction

In the past decade, gold nanoparticles (GNPs) have been intensively studied for their applications in optical devices, biomedical treatments, and sensors[1,2] owing to their unique properties such as surface enhanced Raman scattering (SERS),[3] surface plasmon resonance (SPR),[4] and fluorescence enhancing and quenching effects.[5,6] By tuning their shape-, size-, and surface-dependent properties, the functionalities of GNPs could be greatly broadened.[4,7] Recently, the interplay between GNPs and fluorescent dye molecules is receiving increased attention for the fascinating optical and electronic interactions presented. A number of dye-nanoparticle binary systems have been prepared and investigated.[6,8–10] However, most of them require complicated organic synthesis and the resulting nanoparticles were limited in use since they cannot form homogenous nano composites with their host media. If GNPs can homogeneously mix with dye molecules, this would provide a much easier way to prepare the dye-nanoparticle hybrid system which is in high demand for industrial and technological life use.[7]

For this goal, GNPs are required to be stable and compatible with host functional materials to form homogeneously mixed nano composites. It is established that dispersing GNPs in organic solvents is more appealing compared to dispersing them in water because their low interfacial energies allow for a high degree of control during solution and surface processing. To enhance their stability and compatibility with organic functional media, organo-soluble thiol monolayer-protected GNPs are desirable.[7b,11] Here, decane thiol (n-$C_{10}H_{21}SH$) monolayer-protected gold nanoparticles with varied sizes and shapes were found to be able to homogeneously mix with the strongly fluorescent perylene diimide dye (PDI)[12] in both organic solution and solid state (**Scheme 1**). The particle-dependent properties were investigated by the combination of UV-vis, fluorescence spectra, transmission electron microscopy (TEM), scanning electron microscopy (SEM), and Raman experiments. The gold nanoparticles were found to quench the strong fluorescence of PDI depending on their size and shape.

2. Results and Discussion

Four types of decane thiol monolayer-protected GNPs including three spherical GNPs with different sizes (small, medium and large) and one anisotropic gold nanorod (GNR) as shown in Scheme 1 were synthesized. These four GNPs in CH_2Cl_2 exhibited distinctive SPR absorptions in UV-vis spectra with different solution colors (**Figure 1**). The solution of small GNP_1 showed an SPR peak at 520 nm, the medium GNP_2 showed a peak at 549 nm, and the large GNP_3 showed a peak at 615 nm. The red shift of spherical GNP's SPR accompanying to their size increase was in consistent with previous report.[13] The anisotropic GNR showed the typical absorptions of a transverse SPR peak at 520 nm and a longitudinal peak at 784 nm.[4]

On mixing with the synthesized PDI dye[12b] (Scheme 1) in organic solution (CH_2Cl_2), GNP concentration-dependent UV-vis and fluorescence spectra were depicted in Figure S1. Owing to the organo-soluble and stable n-decane monolayer

Dr. C. M. Xue, Prof. Q. Li
Liquid Crystal Institute and Chemical Physics Interdisciplinary Program,
Kent State University
Kent, Ohio, 44242, USA
E-mail: qli1@kent.edu
Dr. Y. H. Xue, Prof. L. M. Dai
Department of Chemical Engineering
Case Western Reserve University
Cleveland, Ohio, 44106, USA
Dr. A. Urbas
Materials and Manufacturing Directorate
Air Force Research laboratory WPAFB
Ohio, 45433, USA

DOI: 10.1002/adom.201300175

Report Documentation Page

Form Approved
OMB No. 0704-0188

1. REPORT DATE	2. REPORT TYPE	3. DATES COVERED
2013		**00-00-2013 to 00-00-2013**

4. TITLE AND SUBTITLE	5a. CONTRACT NUMBER
Size- and Shape-Dependent Fluorescence Quenching of Gold Nanoparticles on Perylene Dye	5b. GRANT NUMBER
	5c. PROGRAM ELEMENT NUMBER
6. AUTHOR(S)	5d. PROJECT NUMBER
	5e. TASK NUMBER
	5f. WORK UNIT NUMBER
7. PERFORMING ORGANIZATION NAME(S) AND ADDRESS(ES) **Case Western Reserve University,Department of Chemical Engineering,Cleveland,OH,44106**	8. PERFORMING ORGANIZATION REPORT NUMBER
9. SPONSORING/MONITORING AGENCY NAME(S) AND ADDRESS(ES)	10. SPONSOR/MONITOR'S ACRONYM(S)
	11. SPONSOR/MONITOR'S REPORT NUMBER(S)

12. DISTRIBUTION/AVAILABILITY STATEMENT
Approved for public release; distribution unlimited

13. SUPPLEMENTARY NOTES

14. ABSTRACT

15. SUBJECT TERMS

16. SECURITY CLASSIFICATION OF:			17. LIMITATION OF ABSTRACT	18. NUMBER OF PAGES	19a. NAME OF RESPONSIBLE PERSON
a. REPORT	b. ABSTRACT	c. THIS PAGE			
unclassified	**unclassified**	**unclassified**	**Same as Report (SAR)**	**7**	

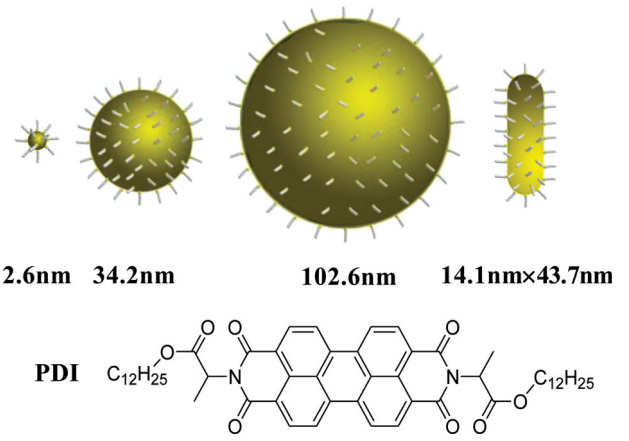

Scheme 1. Chemical structures of PDI and schematic representation of decane-thiol protected gold nanoparticles with different sizes and shapes (sphere and rod).

coated over these GNPs, they were able to disperse well with PDI in CH_2Cl_2. With the addition of GNP, both the UV-vis absorption and fluorescence emission of typical PDI molecule decreased. For the absorption signals of PDI molecules in the UV-vis spectra, they were identical to other PDI molecules showing typical peaks at 526, 490, 459, and 433 nm, corresponding to $v = 0 \rightarrow v' = 0$, 1, 2 and 3 transitions.[14] Compared to free PDI molecules in the lower concentration solution, higher concentration led to different peak shapes due to the existence of partial aggregations of PDI molecules, for example, the ratio of 530 nm peak intensity to 490 nm peak intensity became lower.[14] Based on the UV-vis spectra, the ratio of 526 nm to 490 nm peak was calculated (Table S1). Initially, without adding GNPs, the ratio was 1.30. With the addition of GNPs, all the values increased obviously. The increase of

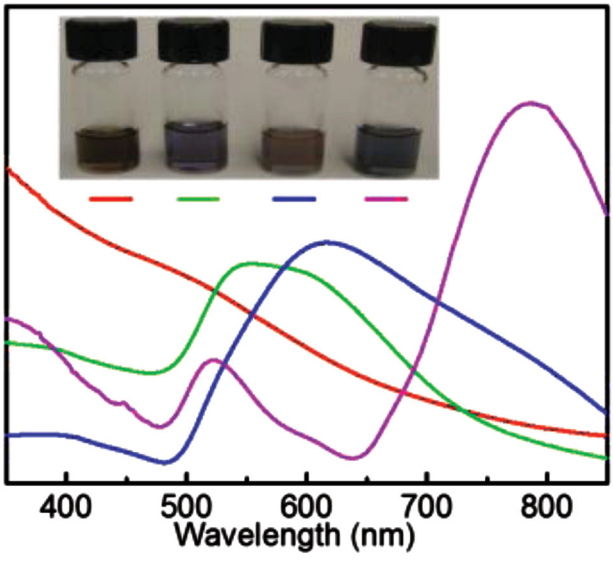

Figure 1. UV-vis spectra of GNP_1 (red curve), GNP_2 (green curve), GNP_3 (blue curve), and GNR (purple curve) in CH_2Cl_2. Inset: the corresponding solutions of the above samples.

the ratio indicated that the aggregations of the PDI molecules in solution were disassembled when GNPs were added. When further increasing the concentration of the nanoparticles, the ratio change was different between spherical GNPs and GNR. For spherical GNPs, when increasing GNP concentration, there was almost no change. For GNR, when increasing its amount, the ratio steadily increased. The adsorption of PDI molecules on the GNP surface could be invoked to explain the decrease of the UV absorption and the peak shape changes. PDI molecules are electron deficient while on the GNP surface the electrons are relatively sufficient.[15] Thus, PDI molecules could be adsorbed on GNPs because of the electronic interactions between PDI molecules and GNP or GNRs. Due to the adsorption, the concentration of PDI molecules in the solutions decreased. Therefore, the solution absorption decreased as PDI molecules were adsorbed onto the GNPs as fewer of them were left in the solution. Meanwhile, due to the concentration reduction, the PDI molecules released from the aggregates into the solution exhibited the spectral signatures of free-state molecules. During the addition of the GNPs, the intensity increase of their typical SPR peaks was also observed in UV spectra, as shown in Figure S2.

For the fluorescence, the signals of all four samples decreased upon the addition of the GNPs. When compared to the UV spectra, the decrease of the intensity of the fluorescence spectra was generally more pronounced. Apart from the adsorption effect discussed above, it has been reported that their fluorescence could be quenched when fluorophores were close enough to GNPs.[5] For the PDI molecules, when they were positioned close to the surface of GNPs, including spherical and rod shapes, the fluorescence was significantly quenched.[6] For the four groups of UV curves, if only there was absorption effect, they would have generated fluoresce curves in a similar decrease way as their corresponding UV curves. However, the decreases of all four groups' fluorescence intensities were much larger and quite different which depended on the type of the added GNPs. Therefore, the significant fluorescence intensity reductions resulted from the quenching effect of the GNPs. Particularly for GNP_1 the intensity was decreased significantly. In the experiment presented here, all shapes and sizes of GNPs studied exhibited quenching of the PDI molecules near their surface in the solution. For the 576 nm peaks, their intensities were compared to the initial PDI solution before adding gold nanoparticles and the ratios were calculated in Table S1 and plotted in **Figure 2**. The fluorescence quenching effect was obviously observed from the color change of the solutions as shown in Figure 2 top. From this graph, different quenching effects related to the GNP size and shape could be discovered. The quenching effect decreased with increasing size of spherical GNPs. The anisotropic GNR, however, had the smallest change even though its size was smaller than the largest spherical GNP_3 and similar to the medium GNP_2. In addition, it is interesting that there were different plasmonic effects of GNPs on PDI fluorescence peaks as shown in Figure S1,. The ratios of the peaks at 576 nm to 626 nm were calculated as listed in Table S2 to explore these effects. During the addition of GNPs, the spherical ones led to ratio reducing while anisotropic GNRs led to ratio increasing. The varied SPR of GNPs may account for such phenomena: as the SPR moved across these peaks, while both peaks would be affected by the proximity of the

Adv. Optical Mater. **2013**,
DOI: 10.1002/adom.201300175

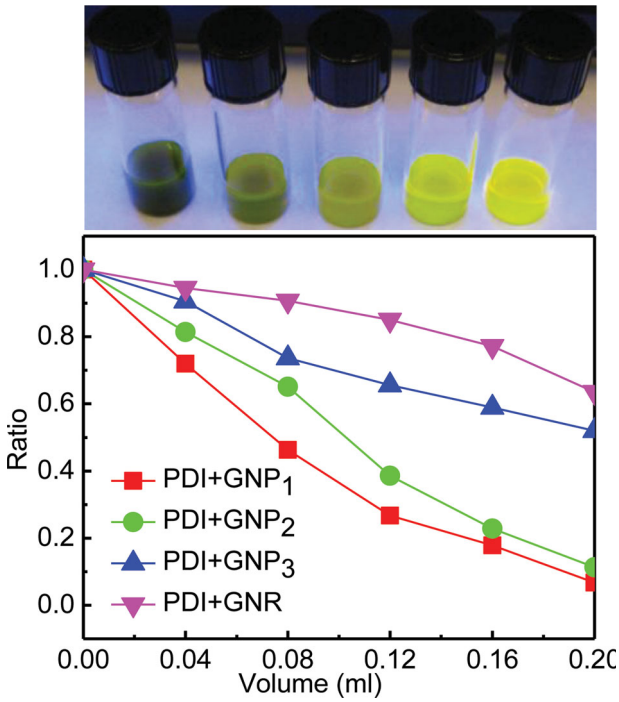

Figure 2. Top: solutions emitting fluorescence under a UV lamp (365 nm) after adding nanoparticles to the PDI solution. From left to right: PDI+GNP_1, PDI+GNP_2, PDI+GNP_3, PDI+GNR and initial PDI. Bottom: the ratio of 576 nm peak of each sample to the initial PDI peak in the fluorescence spectra from Table S1.

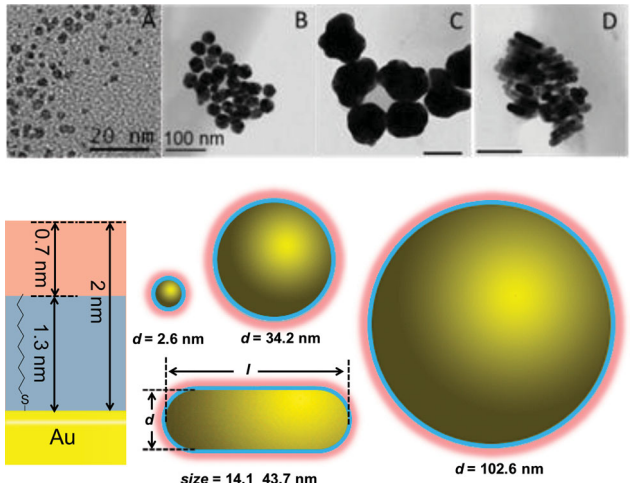

Figure 3. Top: TEM images of the dried solution samples of PDI mixing with gold nanoparticles (A: GNP1, B: GNP2, C: GNP3, D: GNR). The scale bar for B, C, and D are all 100 nm. Bottom: The surface structures of decane thiol monolayer coated gold nanoparticles.

metal surface resulting in intensity reduction, the peaks closer to the SPR would be suppressed more.

Their corresponding TEM images dried from these solution samples are presented in **Figure 3**. Spherical GNPs had varied size from small, medium to large: 2.3 nm (GNP_1), 34.2 nm (GNP_2) and 102.6 nm (GNP_3). The anisotropic GNR had a size of 43.7 nm × 14.1 nm. For each type of GNP, we measured 200 nanoparticles and calculated the average values. For GNP_1 and GNP_2, one value of diameter for each particle was measured. For GNP_3, we took two diameter values for each particle (they were perpendicular to each other) and used their average as the size for this particle. After 200 particles were measured, an average value for GNP_3 was obtained. For GNR, one length value in longitudinal direction and one width value in transverse direction for each particle were taken. The corresponding root-mean-square error (RMSE) values are 0.6 for GNP_1, 4.1 for GNP_2, 10.2 for GNP_3, and 7.2 for GNR length and 4.6 for GNR width. The schematic description of the surface structures of the nanoparticles was also displayed in Figure 3. For GNPs, the most efficient quenching distance was discovered to be about 2 nm.[5] Since the *n*-decane thiol monolayer occupied 1.3 nm thickness, the most efficient quenching region was left open to the PDI molecules. Based on the diameters of the spherical GNPs and the width and length of the GNR, the volume of the four nanoparticles could be obtained (**Table 1**). Since the weight added into the solution was identical (0.02 mg), the number of each kind of nanoparticles could be estimated. As GNP_3 was the largest in size, its number was the smallest. Each type of GNP had its own total quenching volume. The volume surrounding the particle where PDI was efficiently quenched was calculated based on the nanoparticle number, the surface area of each particles, and the surface quenching thickness. The

Table 1. The analysis of quenching effect of gold nanoparticles mixing with PDI in solutions. Concentration for all gold nanoparticles: 0.02 mg/mL, 1 mL solution was taken for calculation.

Sample	d_{core} [nm][a)]	$d_{inert\ layer}$ [nm][a)]	$d_{effective\ layer}$ [nm][a)]	Particle Volume V_p [nm^3][b)]	Particle Numbers (n)[c)]	Particle Quenching Volume V_q [nm^3][d)]	Total Effective Quenching Volumne [nm^3][e)]
GNP_1	2.6	5.2	6.6	9.2	1.1×10^{14}	76.9	8.7×10^{15}(191.7)
GNP_2	34.2	36.8	38.2	20944.9	4.9×10^{10}	3092.9	1.5×10^{14} (3.4)
GNP_3	102.6	105.2	106.6	565511.9	1.8×10^{9}	24663.1	4.5×10^{13} (1)
GNR	14.1×43.7	16.7×46.3	18.1×47.7	8291.3	1.2×10^{11}	1798.8	2.2×10^{14} (5.0)

[a)] d_{core} is the diameter of gold nanoparticle cores; $d_{inert\ layer}$ is the diameter of gold nanoparticles with a decane thiol layer; $d_{effective\ layer}$ is the diameter of the gold nanoparticles with an effective quenching layer; for GNR the size is expressed as d × l (width × length). [b)] The volume of each single gold nanoparticle. For GNP, the volume = $4\pi(d_{core}/2)^3/3$; for GNR, the volume = $4\pi(d_{core}/2)^3/3 + \pi l_{core}(d_{core}/2)^2$. [c)] n = 0.02 mg/[$\rho_{Au} \times V_p$], ρ_{Au} = 19.3 g cm^{-3}. [d)] The effective quenching volume for GNPs = $4\pi[(d_{effective\ layer}/2)^3-(d_{inert\ layer}/2)^3]/3$; for GNR = $4\pi[(d_{effective\ layer}/2)^3-(d_{inert\ layer}/2)^3]/3 + \pi(l_{effective\ layer}-d_{effective\ layer})[(d_{effective\ layer}/2)^2-(d_{inert\ layer}/2)^2]$. [e)] The total effective quenching volume = Vq × n. In the brackets, GNP_3 was set as 1 for easy comparison.

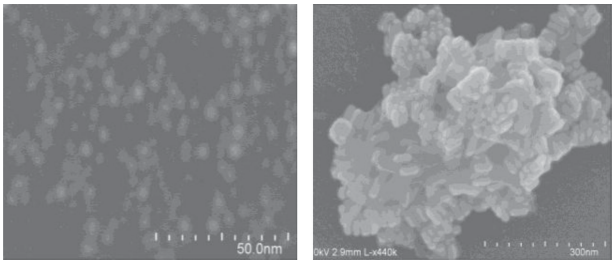

Figure 4. SEM images of dried samples of C_{10}-GNP_1 (left) and C_{10}-GNR (right) in PDI solution on the silicon wafer.

smallest GNP_1 material had the largest total quenching volume. This corresponds well with the decrease of the quenching effect when the particle size increased. In fact, this effect could be even stronger for the small nanoparticles than one which this calculation suggested because the effective quenching distance from the nanoparticle surface increases with the decrease of particle size.[5] Interestingly, the GNR sharing a similar size with GNP_2, exhibited a weaker quenching effect than either the middle or the largest GNP_3. From TEM images, the reason could be the strong aggregation of the GNR due to its particular shape: the sides provided the nanorods more surface area for attractive forces to form self-assemblies.[4,6] As seen from the UV-vis spectra, the longitudinal peak of GNRs have blue shifts upon increasing their concentration in PDI (Figure S2d). With the addition of 0.04 mL, 0.08 mL, 0.12 mL, 0.16 mL and 0.20 mL, the corresponding peak positions were 820 nm, 817 nm, 811 nm, 809 nm, and 800 nm, respectively. This indicated the existence of side-by-side GNR self-assemblies.[16] Also in TEM, GNP_1 were well dispersed in PDI, while GNR exhibited very strong aggregation. More TEM images of side-by-side assembled GNR in PDI were presented in Figure S3. The strong aggregation behavior of GNRs was also confirmed by SEM as displayed in **Figure 4**. For dried solution samples, the GNP_1 was well dispersed without any assembly, but for GNR very clear aggregation occurred. Due to this aggregation behavior, the effective surface volume for quenching was significantly decreased and GNR could exhibit a relatively suppressed quenching effect or lower effective quenching volume compared to the largest GNP_3.

In the solution, GNPs exhibited strong quenching effect on PDI fluorescence, and this effect was further studied for the solid samples. The GNP doped PDI sample solutions (concentration of GNP and PDI: 0.02 mg/mL and 0.8 mg/mL) were spin coated on quartz plates. Their fluorescence spectra are displayed in **Figure 5**. Compared to the initial PDI without GNP doping, the fluorescence intensity ratio at 650 nm were: GNR 0.79, GNP_3 0.38, GNP_2 0.16 and GNP_1 0.07. The results showed the same trend of intensity changes as the solution fluorescence spectra: quenching effect decreased in the sequence of GNP_1, GNP_2, GNP_3 and GNR. This result was consistent with the varied quenching volumes of the GNPs, where the smallest GNP_1 had the strongest quenching effect due to its largest quenching volume. For the GNR, with strong self-assemblies (Figure 3, Figure S3, and Figure 4) after dried, this reduced its quenching volume significantly. For further investigation, the samples were cast onto a soft substrate filter paper, as shown in

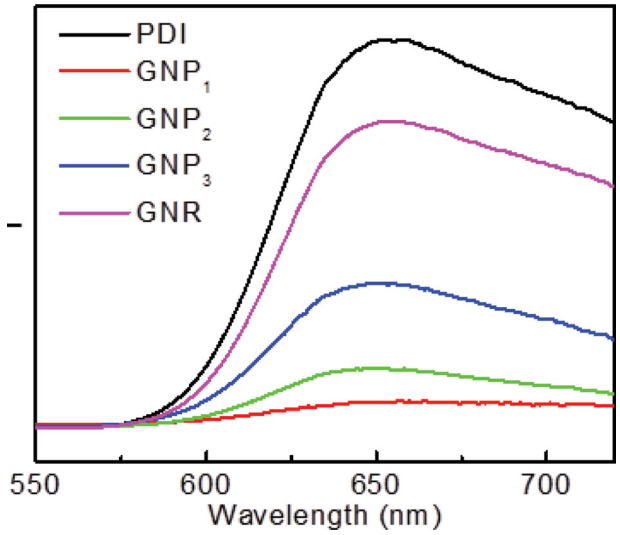

Figure 5. Fluorescence spectra of solid films of mixed solution samples casted on quartz via spin coating. Excitation wavelength: 490 nm.

Figure 6A. For the preparation, the paper samples were dipped in the solutions of PDI mixed with GNPs, and then removed and dried. Under the daylight lamp, the samples with GNP_1 and GNP_2 exhibited a darker color due to the large amount of GNPs. For GNP_3 and GNR, the appearance was the same as the

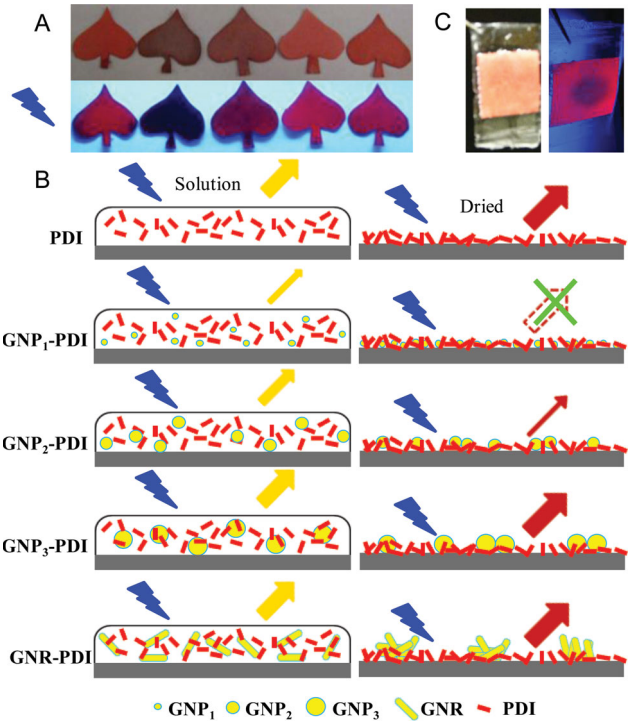

Figure 6. (A) The dried samples under a daylight (top) and under a UV lamp (bottom). (B) The schematic depiction of the molecular state of PDI molecules mixing with GNP_1, GNP_2, GNP_3 and GNR in the solution and solid states. (C) Picture of a PDMS film containing a square piece of filter paper covered by PDI molecules and treated with one drop of low concentration GNP_1. Left: under a daylight lamp; right: under a UV lamp.

Adv. Optical Mater. **2013**,
DOI: 10.1002/adom.201300175

PDI sample without GNPs, a red color. Under a UV lamp, plain PDI displayed dark red fluorescence, the GNP_1 fluorescence was totally quenched, and the GNP_2 was partially quenched. For GNP_3 and GNR, however, they were almost identical to the plain PDI sample.

The above results were schematically presented in Figure 6B. In non-aggregated state in solution, PDI molecules exhibited light yellow fluorescence. During drying from the solution, the PDI molecules tended to aggregate and displayed dark-red color due to aggregation based on strong intermolecular π-π interactions. When PDI molecules were close to GNP, their fluorescence was quenched. The quenching effect depended on gold nanoparticle sizes and shapes. In the experiment, the smallest GNP_1 displayed the strongest quenching effect. This effect decreased in the sequence of GNP_1, GNP_2, GNP_3 and GNR. For the solutions, because there were free PDI molecules far away from the GNPs, significant fluorescence was maintained. Since the quenching effect of GNP_1 was stronger than GNP_2, GNP_3 and GNR in solid state, when the solution dried, the GNP_1 almost completely quenched PDI molecules that no fluorescence was observed. For GNR, although its size was much smaller than GNP_3 and was similar to the medium GNP_2, both of the solution and solid samples displayed stronger fluorescence than other nanoparticles, possibly due to the strong self-aggregation.

Although GNP_1 showed remarkable quenching effect on PDI, the relatively large number of GNP_1 particles gave a darker appearance compared with plain PDI. This reduces the attractiveness of GNP_1 as an anticounterfiting measure. If the amount of GNP_1 significantly decreased so that the appearance under daylight was the same as plain PDI, but it still effectively quenches the PDI under a UV lamp, which would be much more appealing and technologically relevant. To confirm this, a solution of GNP_1 with very low concentration has been used to mix with PDI in solid film (supporting information). Interestingly, the area with GNP_1 could not be observed with naked eyes under the daylight but it exhibited an obvious black spot under a UV lamp due to the strong fluorescence quenching effect. PDMS was further used to seal the sample and the same quenching effect was observed. The picture of the sample is shown in Figure 6C. Apart from filter paper, other soft media such as fabrics could be used as the substrate. This provided insight into practical applications of gold nanoparticles. For example, this could potentially be used in the antifraud and display techniques.

Since GNPs have SERS effect, Raman spectra were studied for the solid samples dried from the mixture solutions. The Raman spectra of the PDI, and PDI mixing with GNP_1, GNP_2, GNP_3 and GNR are shown in Figure S4. There are typical PDI peaks positioned at 1071.0, 1305.0, 1380.4, 1456.4 and 1588.2 cm^{-1}.[17] The SERS enhancement effect of spherical GNPs was weak and only a small enhancement was observed. Among them, the smaller GNP_1 and GNP_2 had a stronger effect than GNP_3. This could be the existence of larger amount of GNP_1 and GNP_2 nanoparticles compared with GNP_3 nanoparticles in the mixture. However, for GNR the enhancement was significantly stronger and the curve showed a smoother shape with much less noise than the others. This is consistent with other report.[18] This would be ascribed to the strong self-assembly of GNRs which provided hotspots for PDI molecules. In addition, the excitation wavelength of the Raman spectroscopy was 785 nm was very close to the longitudinal SPR of GNRs, which might also contribute to this strong enhancement.

3. Conclusion

The organo-soluble thiol monolayer-protected GNPs with different sizes (small, medium and large) and shapes (sphere and rod) mixed with fluorescent PDI dye molecules in both solution and solid states have been investigated. The samples were studied with UV-vis absorption, fluorescence, TEM, SEM and Raman spectroscopy. The fluorescence of PDI molecules mixed with GNPs in both solution and solid was shown to be quenched. The distinctive quenching effects depended on both sizes and shapes of the GNPs. The smallest spherical GNP_1 had the strongest quenching effect, resulting from the largest effective quenching volume. The theoretical calculations were consistent with experimental results. Moreover, the larger GNRs tended to aggregate which reduced quenching volume. With the strongest quenching effect, the smallest GNP_1 nanoparticles were deposited on a PDI solid film. Under daylight, the film showed uniform red color whereas the area with the small GNPs displayed a remarkable black spot under a UV lamp (365 nm). The sample was sealed in a PDMS film which displayed excellent stability and flexibility. This was also environmental friendly and nontoxic since the gold nanoparticles were sealed, prohibiting them from leaving the surface. The combination of fluorescent dyes and GNPs could be used in macroscopic applications such as antifraud technology by inkjet printing. This research may open up a new avenue introducing nanomaterials into practical applications.

4. Experimental Section

Materials and Measurements: All chemicals and solvents were purchased from commercial supplies and used without further purification. $HAuCl_4$ is a 30 wt% in diluted HCl solution. UV-visible spectra were collected on a PerkinElmer Lambda 25 UV-vis spectrometer at the resolution of 1 nm. Fluorescence spectra were recorded on a FluoroMax-3 spectrafluorometer of Horiba scientific at the resolution of 1 nm. For transmission electron microscopy (TEM) observation, solution samples were first dispersed on TEM Cu grids pre-coated with thin carbon film (Cu-400 CN) purchased from Pacific Grid Tech. After completely dried, they were studied using a FEI Tecnai TF20 FEG TEM. Scanning Electron Microscope (SEM) images were obtained by using a Hitachi SU8000 Field Emission SEM. For imaging the gold nanorods, the conditions were: 10 kV accelerating voltage, 2.9 mm working distance, and 10 μA emission current. For imaging the gold nanoparticles, the conditions were: 30 kV accelerating voltage, 7.2 mm working distance, and 7 μA emission current. The Raman spectra are obtained with a RENISHAW inVia Raman microscope instrument using a diode laser with an excitation wavelength of 785 nm. Samples for Raman spectra were casted on silicon wafers and left to dry before measurements. Each spectrum is obtained in 10 s collection time with five accumulations.

Synthesis of Perylene Diimide (PDI): The PDI molecule (*N*,*N*'-di((*S*)-2-dodecyloxy-1-methyl-2-oxoethyl)-3,4:9,10-perylenetetracarboxyldiimide) was synthesized according to the literature.[12b]

Synthesis of Decanethiol Monolayer Protected Small Spherical Gold Nanoparticles (2.3 nm) (GNP_1): The route is based on a literature

procedure[11] with some modifications. An aqueous solution of hydrogen tetrachloroaurate (3 mL, 30 mmol/L) was mixed with a solution of tetraoctylammonium bromide in toluene (8 mL, 50 mmol/L). The two-phase mixture was vigorously stirred until all the tetrachloroaurate was transferred into the organic layer. The water layer was removed and 30 mg decanethiol was then added to the organic phase. A freshly prepared aqueous solution of sodium borohydride (2.5 mL, 0.4 mol/L) was slowly added with vigorous stirring. After further stirring for 3 h the organic phase was separated, evaporated to 1 mL in a rotary evaporator and mixed with ethanol (40 mL). The mixture was kept for 4 h at –18 °C. The crude product was filtered off and washed with ethanol. The solid was dissolved in CH_2Cl_2 and centrifuged at 14000 rpm for 12 min. After centrifuge, the top layer was removed and the solid was sonicated after adding CH_2Cl_2. This wash step was carried several times.

Synthesis of Decanethiol Monolayer Protected Medium Spherical Gold Nanoparticles (34.2 nm) (GNP_2): Firstly, the water-soluble GNPs protected by surfactant were prepared based on the method[19] with some modification. 100 mL of 2.5×10^{-4} M $HAuCl_4$ aqueous solution was heated to 120 °C in an oil bath under vigorous stirring for 30 min. Then, 11 mL of 1% (wt%) sodium citrate aqueous solution was added into the above solution with continued boiling. After 20 min, the solution was cooled. 20 mL of the solution was centrifuged. After removing the top layer solution, the GNP_2 in the bottom was dissolved in the mixture of H_2O (15 mL) and THF (15 mL) accompanied by sonication. 30 mg decanethiol was then added to this solution and it was stirred overnight. After centrifuge, the top layer was removed and the solid was sonicated after adding CH_2Cl_2. This wash step was carried several times.

Synthesis of Decanethiol Monolayer Protected Large Spherical Gold Nanoparticles (102.6 nm) (GNP_3): Firstly, the water-soluble GNPs protected by surfactant were prepared based on the method[18] with some modification. Into a flask was added a 9 mL of the growth solution containing a mixture of 2.5×10^{-4} M $HAuCl_4$ and 0.01 M CTAB. Warming was necessary to dissolve the CTAB. 50 µL of 0.1 M freshly prepared ascorbic acid was added into the flask followed by gentle stirring for 2 min. Finally 0.5 mL of the above Au seed (34.2 nm) aqueous solution was added into the flask, and the mixture was kept at 30 °C in a water bath for at least 6 h. After centrifuge and removing the top layer solution, the GNP_3 in the bottom was dissolved in the mixture of H_2O (15 mL) and THF (15 mL) accompanied by sonication. 30 mg decane thiol was then added to this solution and it was stirred overnight. After centrifuge, the top layer was removed and the solid was sonicated after adding CH_2Cl_2. This wash step was carried several times.

Synthesis of Decanethiol Monolayer Protected Gold Nanorods (GNRs): Firstly, the CTAB-coated GNRs were freshly prepared by the seed-mediated growth method.[4] For seed preparation, specifically, 0.5 mL of an aqueous 0.01 M solution of $HAuCl_4$ was added to CTAB solution (15 mL, 0.1 M) in a vial. A bright brown-yellow color appeared. Then, 1.20 mL of 0.01 M ice-cold aqueous $NaBH_4$ solution was added all at once, followed by rapid inversion mixing for 2 min. The solution developed a pale brown-yellow color. Then, the vial was kept in a water bath maintained at 25 °C for future use. For nanorods growth, 9.5 mL of 0.1 M CTAB solution in water was added to a tube, 0.40 mL of 0.01 M $HAuCl_4$ and 0.06 mL of 0.01 M $AgNO_3$ aqueous solutions were added in this order and mixed by inversion. Then, 0.06 mL of 0.1 M of ascorbic acid solution was added and the resulting mixture at this stage becomes colorless. The seed solution (0.02 mL) was added to the above mixture tube, and the tube was slowly mixed for 10 s and left to sit still in the water bath at 25–30 °C for 3 h. The final solution turned purple within minutes after the tube was left undisturbed. The solution of CTAB-GNRs was centrifuged at 7500 rpm per 20 min several times to remove the excessive CTAB and other solution components and redispersed in 1.5 mL of water. Then, this aqueous solution of GNRs was added dropwise to a solution of the decanthiol (30 mg) in THF (40 mL) with stirring. The color of the reaction mixture is purple. The reaction mixture was continued to stir at room temperature for 3 days and then centrifuged. To improve the GNRs with thiol molecules over the surface, the precipitates were dispersed in CH_2Cl_2 and sonicated, 10 mg decanethiol were added into the solutions. The solution was stirred for another 24 h and centrifuged. This procedure was repeated another three times. The as-prepared GNRs were centrifuged and washed with CH_2Cl_2 several times until there was no IR signal in the top layer solution, which means there were no free thiols in the system.

Preparing Solutions of PDI Mixed with GNP/GNR: 1mg/mL PDI CH_2Cl_2 solution was first prepared. For gold nanoparticle solutions, each solution was made in CH_2Cl_2 contains 0.1 mg/mL. For the mixtures, 0.2 mL gold nanoparticle was slowly added into 0.8 mL PDI solution and swirled vigorously. There solutions were sealed for test. Before each experiment, each was sonicated for 2 min before use. For UV experiment, since the absorption of these solutions was very strong, 1 mm light path UV cell was used.

Preparing a PDMS Film to Seal the Solid PDI and GNP_1 Sample: After cast one drop of 2.6 nm GNP_1 (0.002 mg/mL) on a square piece of filter paper, it was dipped in PDI solution. Then it was lift and dried. The sample was transferred to a glass slide pretreated with a thin layer of liquid PDMS with 20% crosslinker. After another layer of liquid PDMS was cast on, it was aging at 60 °C for 2.5 h in a vacuum oven. Then the flexible film was removed from the glass slide. The thickness was about 1 mm.

Supporting Information

Supporting Information is available from the Wiley Online Library or from the author.

Acknowledgements

This work was supported by the Air Force Office of Scientific Research (AFOSR FA9550–09–1–0254). This work was performed in part at the University of Michigan Lurie Nanofabrication Facility, a member of the National Nanotechnology Infrastructure Network, which is supported in part by the National Science Foundation. Assistance from Dr. V. Ray for SEM was acknowledged. With assistance from Dr. M. Gao, the TEM data were obtained at the (cryo) TEM facility at the Liquid Crystal Institute, Kent State University, supported by the Ohio Research Scholars Program Research Cluster on Surfaces in Advanced Materials. Prof. Q. Wei is thanked for the helpful discussion.

Received: April 18, 2013
Revised: May 22, 2013
Published online:

[1] M. C. Daniel, D. Astruc, *Chem. Rev.* **2004**, *104*, 293.
[2] N. J. Halas, S. Lal, W. S. Chang, S. Link, P. Nordlander, *Chem. Rev.* **2011**, *111*, 3913.
[3] S.-Y. Chen, J. J. Mock, R. T. Hill, A. Chilkoti, D. R. Smith, A. A. Lazarides, *ACS Nano* **2010**, *4*, 6535.
[4] C. J. Murphy, T. K. San, A. M. Gole, C. J. Orendorff, J. X. Gao, L. Gou, S. E. Hunyadi, T. Li, *J. Phys. Chem. B* **2005**, *109*, 13857.
[5] P. Anger, P. Bharadwaj, L. Novotny, *Phys. Rev. Lett.* **2006**, *96*, 113002.
[6] C. M. Xue, O. Birel, M. Gao, S. Zhang, L. M. Dai, A. Urbas, Q. Li, *J. Phys. Chem.C* **2012**, *116*, 10396.
[7] a) S. Eustis, M. A. El-Sayed, *Chem. Soc. Rev.* **2006**, *35*, 209; b) J. M. El Khoury, X. Zhou, L. Qu, L. Dai, A. Urbas, Q. Li, *Chem. Commun.* **2009**, 2109; c) Y. Li, D. Yu, L. Dai, A. Urbas, Q. Li, *Langmuir* **2011**, *27*, 98.
[8] C. M. Xue, Y. Q. Xu, Y. Pang, D. S. Yu, L. M. Dai, M. Gao, A. Urbas, Q. Li, *Langmuir* **2012**, *28*, 5956.
[9] T. Hasobe, H. Imahori, P. V. Kamat, T. K. Ahn, S. K. Kim, D. Kim, A. Fujimoto, T. Hirakawa, S. Fukuzumi, *J. Am. Chem. Soc.* **2005**, *127*, 1216.
[10] S. Vukovic, S. Corni, B. Mennucci, *J. Phys. Chem. C* **2009**, *113*, 121.

[11] a) M. Brust, M. Walker, D. Bethell, D. J. Schiffrin, R. Whyman, *Chem Commun.* **1994**, 801; b) X. Zhou, J. M. El Khoury, L. Qu, L. Dai, Q. Li, *J. Colloid Interf. Sci.* **2007**, *308*, 381.
[12] a) F. Wurthner, *Chem. Commun.* **2004**, 1564; b) Y. J. Xu, S. W. Leng, C. M. Xue, R. K. Sun, J. Pan, J. Ford, S. Jin, *Angew. Chem. Int. Ed.* **2007**, *46*, 3896.
[13] S. Link, M. A. El-Sayed, *J. Phys. Chem. B* **1999**, *103*, 8410.
[14] W. Wang, J. J. Han, L. Q. Wang, L. S. Li, W. J. Shaw, A. D. Q. Li, *Nano Lett.* **2003**, *3*, 455.
[15] M. Walter, J. Akola, O. Lopez-Acevedo, P. D. Jadzinsky, G. Calero, C. J. Ackerson, R. L. Whetten, H. Gronbeck, H. Hakkinen, *Proc. Natl. Acad. Sci. USA* **2008**, *105*, 9157.
[16] H. S. Park, A. Agarwal, N. A. Kotov, O. D. Lavrentovich, *Langmuir* **2008**, *24*, 13833.
[17] C. A. Jennings, G. J. Kovacs, R. Aroca, *Langmuir* **1993**, *9*, 2151.
[18] B. Nikoobakht, J. P. Wang, M. A. El-Sayed, *Chem. Phys. Lett.* **2002**, *366*, 17.
[19] Y. J. Huang, D. H. Kim, *Langmuir* **2011**, *27*, 13861.